



Journal of Applied Sciences

ISSN 1812-5654

science
alert

ANSI*net*
an open access publisher
<http://ansinet.com>

Experimental Investigations Water Surface Characteristics in Strongly-Curved Open Channels

A.A. Akhtari, J. Abrishami and M.B. Sharifi

Department of Civil Engineering, Ferdowsi University of Mashhad, 91775-1111, Iran

Abstract: To study water surface characteristics in strongly-curved bends in open channels, a flume was constructed at hydraulic laboratory of Ferdowsi University of Mashhad and was fully calibrated in several stages. The experiments could be carried out on 30, 60 and 90° strongly-curved bend. Dictating conditions of strongly-curved bend, a ratio of curvature radius to channel width was chosen to be 1.5. Experiments were carried out on each bend with the given radius of curvature, considering at least 5 constant discharge values and extensive data were collected. Analyses of the data showed that in a distance equal to channel width from the bend entry and bend exit, water surface is not affected by bend. Also, the ratio of super-elevation at bend entry and bend exit, to the downstream depth are not function of discharge and are almost constant for a bend with a given angle of curvature. Study of water surface at internal sections of bend revealed that in strongly-curved bends, water surface does not have a linear profile and the transversal slope in these sections which are close to the inner bank in bend is rather much greater in comparison with outer bank. To evaluate change of water surface, a new equation is represented.

Key words: Laboratory, open channel, strongly-curved, super-elevation, water surface, tangential velocity

INTRODUCTION

It is observed in investigating of velocity component in bends that observed helical flow at bend by adding pigments to water. This helical flow is formed by secondary currents. It is stated that a secondary current occurs due to imbalance between centrifugal forces and pressure gradient induced forces at surface. In other words, close to the inner bank and also at channel bed, pressure gradient exceeds centrifugal forces and conveys water in transverse direction toward the inner bank. At free surface, centrifugal forces drive flow to the outer bank. This kind of flow is called secondary current (Lien *et al.*, 1999).

Rozovskii (1957) worked on rectangular channels with 180° bend in completely smooth and rough beds. Channel width was 80 cm and bend radius of curvature on the centerline was assumed to be 80 cm, so a ratio of $R_c/b = 1$ was chosen where, R_c was the radius of curvature and b was the width of channel. Discharge value of 12.3 L sec⁻¹, flow depth of 5.8 cm, Froude number of 0.35 and Reynolds number of 14000 were selected. He also, performed an extensive research on trapezoidal channels. He illustrated the changes of the tangential velocity distribution at transversal direction and spelt out the cause of generation and intensification of the secondary

current through the bend. In these studies no researches were fulfilled on water surface transversal profile at bend entry and bend exit in strongly-curved open channels, also on its varieties through bend.

Engelund (1974) described the theory of helical flow in circular bends for a wide rectangular open channel.

Leschziner and Rodi (1979) represented a numerical model in conformity with Rozowski tests on a 90° strongly-curved bend with a ratio of average radius to width equal to 1. In that investigation he didn't reach to a linear surface slope at cross section but in both numerical investigation and laboratory model, surface slope near inner bank was obtained greater than external bank.

De Vriend (1979) carried out experiments on a 180° bend, which was one of his investigations on a bend at University of Delft, Netherlands. This bend had rectangular cross section with a width of 1.7 m and central radius of 4.25 m. The lengths of straight channel before and after bend were 6 m. Flow discharge for this test was 190 L sec⁻¹ and flow depth for downstream channel was 0.18 with Froude number of 0.215. De Vriend and Geoldof (1983) worked on another model with central angle of 90°, discharge of 0.61 m³ sec⁻¹, width of 6 m, depth of 0.25, 50 m radius of curvature and Froude number of 0.25. In these studies the water surface transversal profile through

the bend was linear but water surface elevation was not calculated at upstream and downstream of the bend.

Steffler (1985) studied a channel with 270° central angle. This channel had rectangular cross section with width of 1.07 m and depth of 0.2 m. The central radius of curvature is considered to be 3.66 m. Two conditions were considered, one with depth of 6.1 cm and the other with depth of 8.5 cm and bed slope of 0.00083. He presented a new 2D numerical model based on depth-averaged velocity, such that the secondary current having 3D nature was involved and evaluated validity of the model by comparing the numerical and experimental results. After surveying the experimental and numerical results, water surface transversal profile was calculated linear and he didn't comment on it concerning its quantity at bend entry and bend exit.

Anwar (1986) worked on 31 and 180° bends with natural-topography beds. Shimuzu *et al.* (1990) assumed a logarithmic vertical distribution of the longitudinal velocity and developed a 3D hydrodynamic model. Molls and Chaudhry (1995) developed a 2D depth-average model to solve unsteady flow in open channel.

Ye and McCorquadale (1998) worked on two test cases, one was a 270° bend with a one-sided trapezoidal cross section and Froude number of 0.475 and the other was a meander bend consisted of two 90° bends with a width of 2.34 m and central radius of 8.53 m. Length of straight part between two bends was 4.27 m and length of straight approach channels to the bend were 2.13 m. In this research water depth and approach velocity at entry are assumed to be 0.115 m and 0.366 m sec⁻¹, respectively. By comparison of 3D hydrodynamic simulation based on k-ε model and investigation of the experimental results, they found out that the secondary current and super-elevation begin upstream the bend and gradually reach the bend. Although, they studied on the water surface longitude profile in inner and outer bank and the axis of bend, they didn't comment on the water surface transversal profile, the beginning and end of super elevation position and effect of transversal distribution of tangential velocities on super-elevation.

Blanckaert and De Vriend (2003) also studied a 120° bend, 0.4 m width and central radius of 2 m. However the channel bed was fixed in that research, but using sand with an average grain size of 2.1 mm enabled testing with moveable bed.

Bodnar and Prihoda (2006) presented numerical simulation of turbulent free-surface flow accordance with finite-volume method by SST k-ω turbulence model and analyzed strongly-curved bend with 90° angle. In that study, he calculated the nonlinear slope of water surface in the bend.

According to investigations of Rozovskii (1957), Leschziner and Rodi (1979), if the ratio of bend radius to the channel width was less than 3, bend was considered strongly curved, otherwise it was mild. Since, the aim of this study was to investigate flow pattern in strongly-curved bends, the ratio of central bend radius to the channel width is chosen to be 1.5. Respecting to survey of other studies, it was destined that in most studies water surface transversal profile, situation of the variation of water surface at upstream and downstream due to existence the bend hasn't been surveyed and the effect of transversal distribution of tangential velocities on super-elevation hasn't been calculated. In this research, laboratorial study has been done to evaluate variation of super elevation of the flow at upstream, entry, cross sections, exit and down stream the bend in a strongly curved open channel with different curve angles and different discharges. In addition, the effect of transversal tangential velocity distribution on super elevation was investigated.

Flume characteristics: A laboratorial flume was designed, as illustrated in Fig. 1. The flume has a square section with 403×403 mm² dimensions. Flume side walls and bed were made of Plexiglas, in order to provide the possibility of changing bend direction and observation of the flow characteristics as well. At channel entry, a storage reservoir made of galvanized sheets with dimensions of 150×100×50 cm, was constructed. The function of this reservoir was to convey pumped water from main reservoir to the channel entry. At the conjunction of pumping pipe to the reservoir pressure-reducing baffles were erected perpendicular to the connecting pipes, same as in the USBR stilling basin type VI (Mays, 1999).

Five plastic bar screens perforated to an aluminum bar screen were used to reduce velocity head and create an evenly distributed homogeneous flow in the entry reservoir. To improve developed flow conditions in channel, having no influence of entry conditions on bend and better adaptation of flow lines with the channel, an elliptical transition was used at the connection of channel to reservoir, according to the following equation (USBR, 1985).

$$\frac{x^2}{40^2} + \frac{y^2}{26.4^2} = 1.0 \quad (1)$$

where, x and y values are in centimeters. The larger half-diameter of ellipse is 40 cm, equal to channel width and the smaller half-diameter is equal to two third (2/3) of channel width.

After installation of entrance transition according to Fig. 2, a 3.6 m straight channel made of Plexiglas was

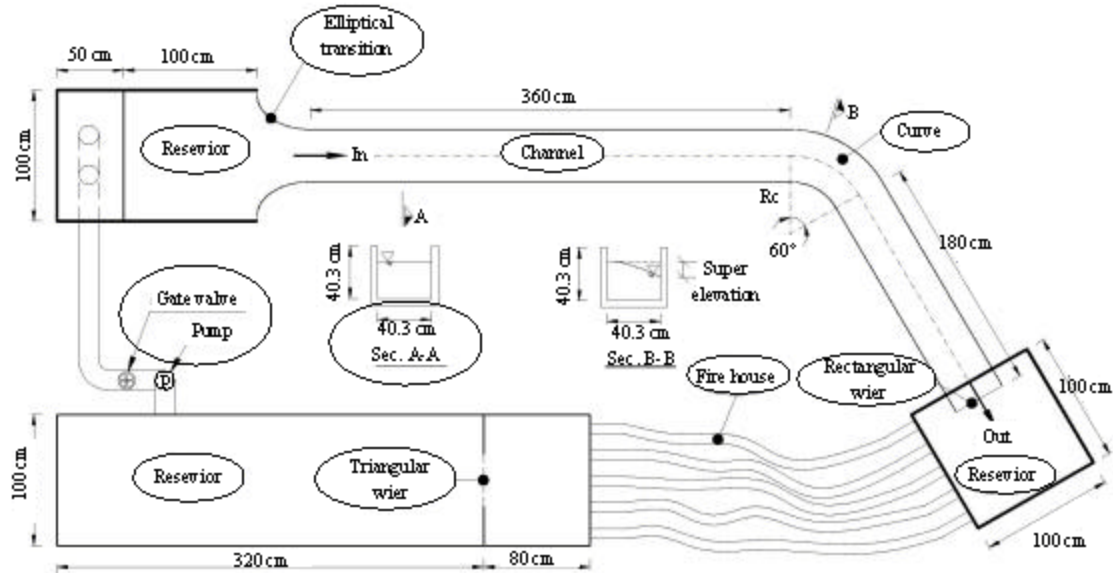


Fig. 1: Plan of experimental flume with 60° bend



Fig. 2: Channel photo at upstream of bend

added to bend entry to provide sufficient expanding-length before the bend. Three bends with central angles of 30, 60 and 90° were connected to the channel separately. After completion of experiments on each bend, the new bend was replaced.

Right after the bend, there was a 1.8 m length straight channel; at the end of this channel a rectangular sharp crested weir was constructed in a way that water surface and velocity variations at weir wouldn't affect the bend. When water passes the weir, pours into a collecting

reservoir with dimensions of 1×1×1.25 m. At reservoir entry a 1×1 m mesh with 1 mm openings was installed. This resulted in energy loss and water diffusion at the end of flume.

To calculate discharge value, a triangular weir with central angle of 90°, was utilized. This weir was placed in main reservoir with dimensions of 1×1×4 m; 0.80 m of which allocated to weir and the remaining 3.2 m was allocated to storage reservoir (which should have a volume, greater than volume of circulating water). A

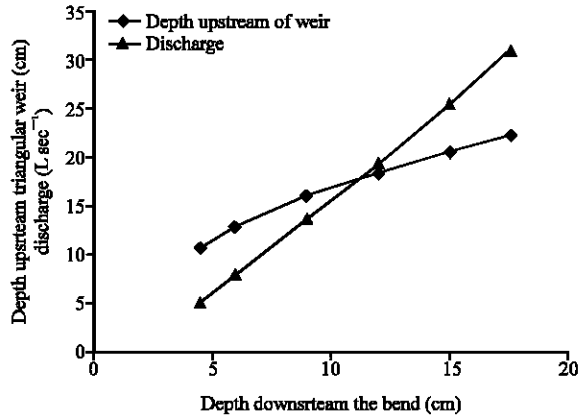


Fig. 3: Values of water discharge and water depth upstream triangular weir

centrifugal pump was used for pumping water from storage reservoir into the flume entry. Flow discharge was regulated by a gate valve with diameter of 150 mm which was installed right after the pump.

To measure velocity and depth values a Vernier ruler was utilized and enabled depth measurement with accuracy of 1 mm in transverse direction and 0.1 mm downward to depth direction. Velocity was measured by a propeller velocity-meter in a range of 2.5 to 150 cm sec⁻¹. Accuracy of this velocity meters based on manufacturer's catalog was as follow:

$$\begin{aligned}
 2.5 < V < 7.5 \text{ cm sec}^{-1} &\rightarrow \text{Error} = 5\% \\
 7.5 < V < 15 \text{ cm sec}^{-1} &\rightarrow \text{Error} = 2\% \\
 15 < V < 150 \text{ cm sec}^{-1} &\rightarrow \text{Error} = 1\%
 \end{aligned}
 \tag{2}$$

Discharge and water depth range: To study flow in strongly curved open channel in different conditions, flow depth and the discharge must be constant at downstream of the channel. In this study, variations in gate valve opening has changed water elevation upstream of the triangular weir and a fixed depth yields a constant discharge during experiment. Water depth of downstream straight channel is also adjusted by changing height of sharp-crested weir installed at downstream of straight channel. In all cases, depth is measured within a distance of 80 cm downstream of the bend and is constant with measurement error, less than 0.5 mm. Values of water depths in straight channel downstream of the bend and depths upstream triangular weir and applied discharges during the experiments are shown in Fig. 3.

Study of water surface elevations in 30, 60 and 90° strongly-curved bends

Super-elevation upstream and downstream of the bend: In this investigation water surface elevation was studied 40 cm upstream and downstream of the bend.

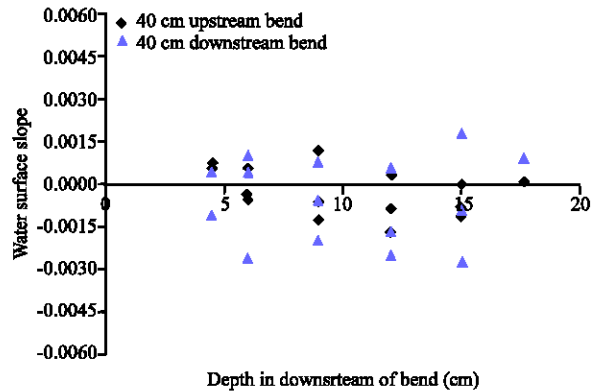


Fig. 4: Water surface slopes dispersion for different depths at 40 cm upstream and downstream of the bend

Water surface slopes at these cross sections for three bends with 30, 60 and 90° angles and for different values of discharges were measured and results are shown in Fig. 4.

It is obvious that in a distance equal to channel width upstream and downstream of the bend, with any central angle of 90° or less, water surface slopes are very closed to zero. Small positive and negative values for water surface slopes, illustrates that water surface is not a function of the discharge and the bend angle.

As shown in Table 1, laboratory data and their statistical distributions with upper limit of values of water surface slopes and their probabilities were calculated. Based on different statistical distributions, for a 99.5% probability, water surface slope at upstream of bend are less than 0.002. For the downstream of bent with 99.5% probability, water surface slope are less than 0.0037.

As shown in Fig. 4 and Table 1, water surface slope, dispersion in both sections is almost zero, so these sections are not affected by bend and different discharges.

Water surface variation at bend entry and bend exit: In this study laboratory investigations on water surface transversal profile at bend entry and bend exit have been surveyed. Water surface profile at bend entry and bend exit were studied for bends of 30, 60 and 90° with central radius of 60 cm. The difference between water levels at the outer and inner bank of the channel is called super-elevation or banking. Measured super-elevation values at bend entry and bend exit were normalized by dividing by downstream average depth in distance of 80 cm after the bend. Analyses on these dimensionless parameters with different downstream water depths and channel discharges, revealed no correlation between water depth and channel discharge and dimensionless super-elevation

Table 1: Water surface slope at 40 cm upstream and downstream of the bend

Position	Event's probability (%)	Mean	Normal distribution	3 parameter normal distribution	Pearson distribution
40 cm upstream the bend	99.5	0.00021	0.0020	0.0020	0.0020
40 cm upstream the bend	99.0	0.00021	0.0018	0.0018	0.0017
40 cm downstream the bend	99.5	0.00046	0.0037	0.0040	0.0042
40 cm downstream the bend	99.0	0.00046	0.0033	0.0035	0.0036

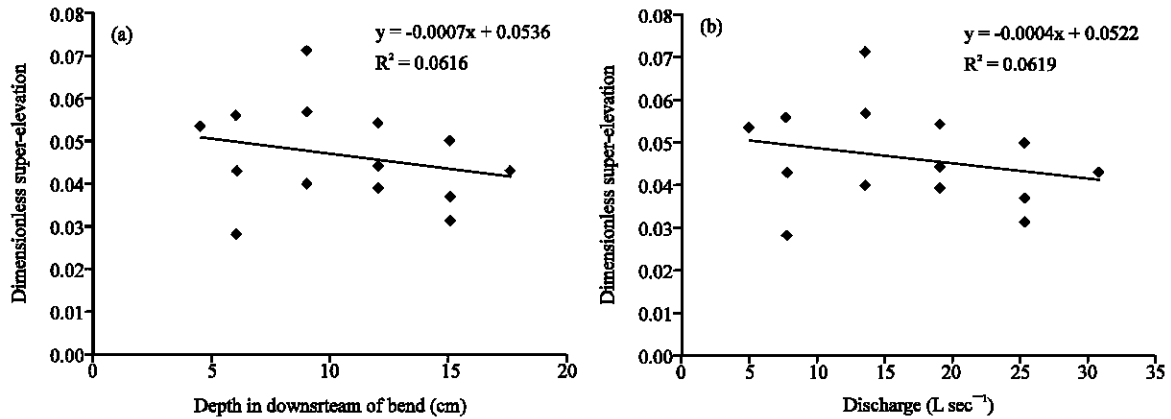


Fig. 5(a, b): Channel depth and discharge Influence on dimensionless super-elevation at bend entry

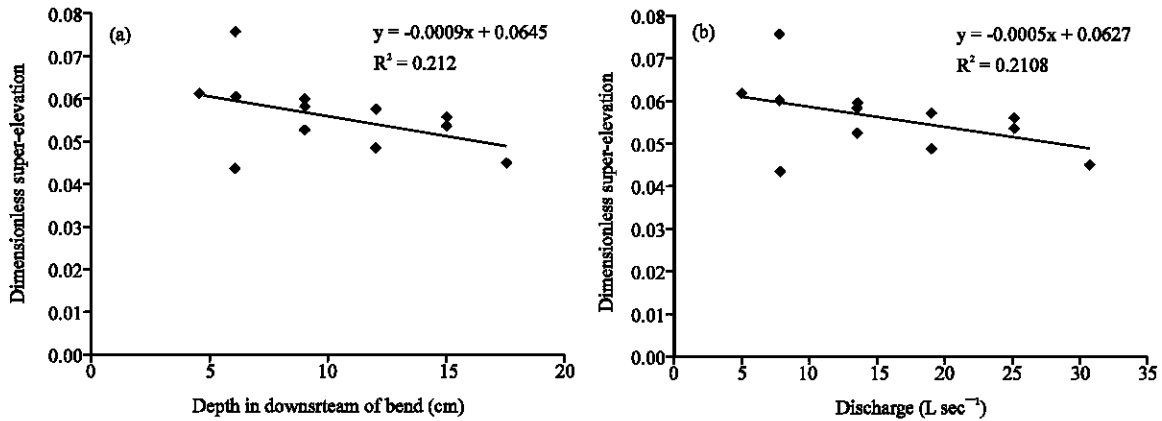


Fig. 6(a, b): Channel depth and discharge Influence on dimensionless super-elevation values at bend exit

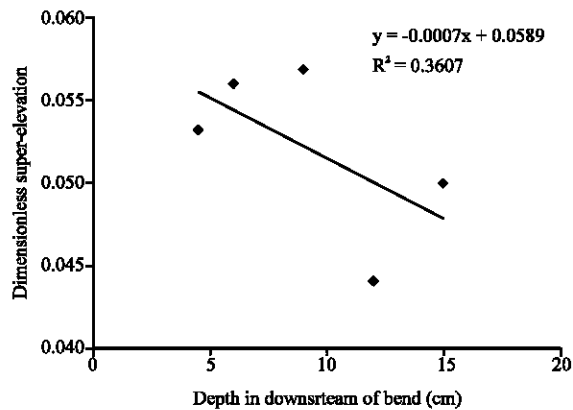


Fig. 7: Influence of water depth in channel on super-elevation values at the entry of 90° bend

values at bend entry and bend exit. As shown in Fig. 5a,b and 6a,b, for all angles at bend entry, dimensionless super-elevations are independent from discharge and downstream depths.

Mean values of dimensionless super-elevation at bend entry and bend exit were 0.0462 and 0.055, respectively. In this phase laboratory data for 30, 60 and 90° bends were analyzed separately and again it was found that the super-elevation is not a function of discharge and downstream channel depth but it is a function of channel curve angle and decreases by reduction in bend curvature angle. For example changes of dimensionless super-elevation with flow depths are schemed in Fig. 7 for 90° bend.

Poor correlation between dimensionless super-elevation values and flow depths revealed no

Table 2: Dimensionless values of super-elevation at bend entry

Angle	Average	90% probably	95% probably	99.5% probably
90°	0.0521	0.0559	0.0559	0.0561
60°	0.0457	0.0548	0.0574	0.0640
30°	0.0345	0.0416	0.0430	0.0465

Table 3: Dimensionless values of super-elevation at bend exit

Angle	Average	90% probably	95% probably	99.5% probably
90°	0.061	0.0717	0.0748	0.0826
60°	0.0532	0.0619	0.0648	0.0727
30°	0.0429	0.0568	0.0591	0.0652

relationship between these quantities. In Table 2 and 3 mean values of dimensionless super-elevation for each curvature angle at bend entry and bend exit are given. For each series of tests with aforementioned angles, normal, log-normal, 3-parameter normal, Pearson type III and log-Pearson type III, probability distributions were fitted. Normal distribution was the best fitted model. Predicted values for 90, 95 and 99.5% probability are given in Table 2 and 3. Water surface at bend entry and bend exit increased as curvature angle changes from 30 to 90°. Average values of dimensionless super-elevation in the bend entry and bend exit change from 0.034 to 0.052 and from 0.0499 to 0.061, respectively. Variation of dimensionless super-elevation at the bend entry and bend exit, as a function curvature angle is given in Fig. 8.

The fitted parabolic equations of Fig. 8 for bend entry and bend exit are as Eq. 3 and 4:

$$\frac{\Delta y}{\bar{y}_{80}} = -0.8 \times 10^{-5} \theta^2 + 0.0013\theta \quad R^2 = 0.99 \quad (3)$$

$$\frac{\Delta y}{\bar{y}_{80}} = -10^{-5} \theta^2 + 0.0016\theta \quad R^2 = 0.98 \quad (4)$$

where, θ is the curvature angle (in degrees), Δy is the difference between water levels at inner and outer bank and \bar{y}_{80} is the average depth at downstream of the channel. In Eq. 3 and 4, correlation of determination of 0.99 and 0.94 were determined for entry and exit of bend.

Non-linear transversal water surface profile in bends: As previously discussed in introduction, most of researchers assumed a linear equation for water surface. In this study, according to the well known Eq. 5, for water surface gradient, mentioned in most open channel flow reference books like Henderson (1966), Subramanya (1982) and Hosseini and Abrishami (1999) a nonlinear transversal water surface profile was derived:

$$\frac{dh}{dn} = \frac{v^2}{rg} \quad (5)$$

where, h denotes water height relative to a reference point, like channel bed and v denotes average velocity for

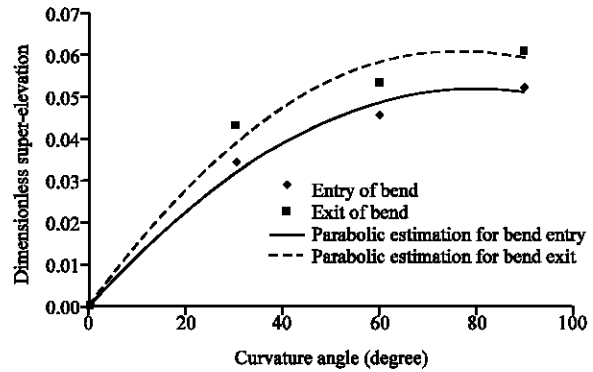


Fig. 8: Effect of curvature angle dimensionless super-elevation

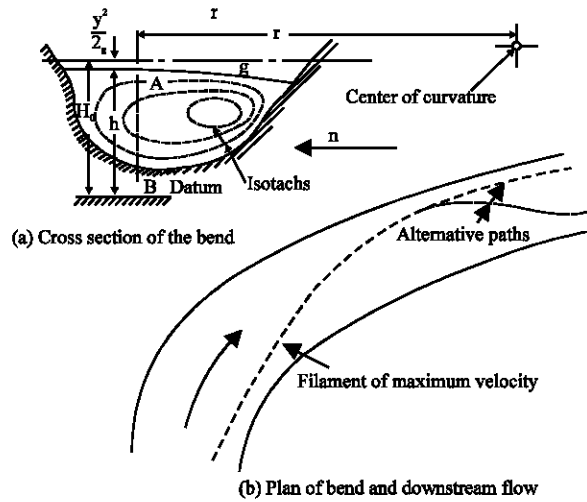


Fig. 9: Flow in plan and cross section of a curved channel (Henderson, 1966)

any vertical section, like AB shown in Fig. 9a and b, r denotes the curvature radius in plan of bed and n is the vertical axis outward the bend. If the bend is a part of a circle as in this work, all vertical vectors of n cross the center of curvature.

In Eq. 5, with large values of curvature radius and small value of velocity, water surface gradient (dh/dn) would be very small and negligible. However in channels with small radius of curvature as in strongly-curved bends, non-uniform transversal distribution of tangential velocity, water surface gradient (dh/dn) wouldn't be constant. Therefore, a nonlinear water surface profile is expected and will be derived later.

Centrifugal forces incline water surface and at half outer-side of the bend cross section water surface rises, which causes velocity decrease in the sub critical flow. In half inner-side of the bend cross section a depression in water surface occurs and hence velocity increase.

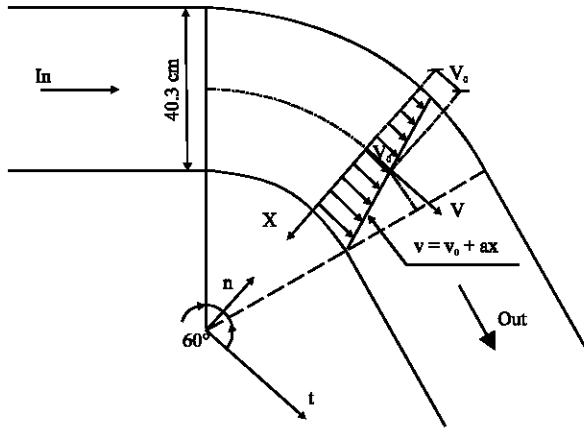


Fig. 10: Plan view of bend coordinates used in Eq. 9

Investigations on 30, 60 and 90° bends with constant downstream depths of 4.5, 6, 9, 12 and 15 cm, showed that from bend entry up to bend exit, where secondary current intensify, velocity distribution in all layers parallel to channel bed very linearly as shown in Fig. 10. Considering Linear distribution of velocity in channel width, velocity decreases close to outer bank and increases near inner bank. Since, curvature radius of outer bank is greater than the radius of inner bank so water surface gradient changes in transversal direction. So, water surface gradient will be larger near the inner bank because of large average tangential velocity and small curvature radius compared to the gradient near the outer bank.

In this research, tangential velocity and water depth profiles were measured for 30° bend at the entry, middle point and end of the bend, while for 60° bend at cross section with central angles of 10, 20, 30, 40, 50 and 60° and for 90° bend cross section with central angles of 0, 22.5, 45, 67.5 and 90°. Tangential velocity were measured, at different layers parallel to the channel bed, in all depths of 4.5, 6, 9, 12 and 15 cm thickness of layers were in the range of 1.5 to 3 cm. Depth average velocity profile was derived by calculating mean velocities in depth. The velocity profile coincides with the linear distribution formula given in Eq. 6.

$$v = V_0 + ax \tag{6}$$

where, a and V_0 are the regression coefficients of depth average velocities.

Considering linear distribution of velocity with curvature radius and using the following variable transformation as shown in Fig. 10, integration of Eq. 5 will result in the Eq. 9.

$$R = R_c - x \tag{7}$$

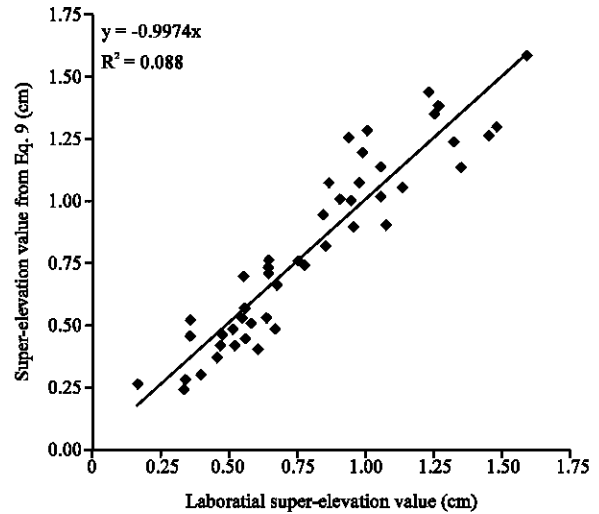


Fig. 11: Calculated super-elevation versus experimental super-elevation in strongly curved channel

$$dn = -dx \tag{8}$$

$$\Delta h = \int_{-\frac{b}{2}}^{\frac{b}{2}} \frac{-(V_0 + ax)^2}{g(R_c - x)} dx = \frac{ab}{g} \{ (aR_c + 2V_0) + (aR_c + V_0)^2 \log(1 - \frac{2b}{b + 2R_c}) \} \tag{9}$$

where, x denotes distance of each point in transversal direction relative to channel axis. R_c is the central radius of curvature and b is the channel width which is equal to 60 and 40 cm, respectively.

V_0 and a regression coefficients with R^2 greater than 0.9, determined from experimental results of transversal distribution of tangential velocities were substituted in Eq. 9. The difference between water elevations at outer and inner bank were measured for each cross section and each discharge. Calculated super-elevations from Eq. 9 are plotted against experimental super-elevations in Fig. 11.

As shown in Fig. 11, linear regression line and coefficient of determination are as follows:

$$y = 0.9974x \quad R^2 = 0.88 \tag{10}$$

The slope of regression line is very close to 1 which shows that experimental results have closely been simulated by Eq. 9.

CONCLUSION

Based on laboratory investigations on 30, 60 and 90° bends in a strongly curve open channel, following results were obtained:

- Within a distance equal to the channel width at upstream and downstream of the bend, water surface is not affected by bend and follows conditions of upstream and downstream of straight channel
- At bend entry and bend exit, dimensionless values of super-elevation are not a function of flow depth and discharge and are only a function of curvature radius. For a determinate central angle, the aforementioned quantity can be computed from Eq. 3 and 4
- In strongly-curved bends, water surface can not be assumed linear due to non-uniform velocity distribution and influence of curvature radius, for prediction of super-elevation in strongly curve channel presented a new equation

ACKNOWLEDGMENT

The authors wish to express their gratitude to Dr. Mohamad Reza Jafarzadeh for his comments and suggestions in constructing the laboratorial model.

NOTATIONS

The following symbols are used in this study:

- a = Regression coefficient for tangential velocity
- B, b = Width of channel
- dh/dn = Water surface gradient
- g = Gravitation acceleration
- h = Local depth of flow
- n = Vertical vector
- q = Discharge
- r, R_c = Radius of curve
- R^2 = correlation coefficient
- v = tangential velocity, velocity
- V_0 = Regression coefficient for tangential velocity
- x = Coordinate direction
- y = Coordinate direction
- y = Depth of flow
- \bar{y}_{80} = Downstream average depth in distance of 80 cm after bend
- Δy = Difference of water depth between internal and outer banks
- θ = Curvature angle

REFERENCES

Anwar, H.O., 1986. Turbulent structure in a river bed. *J. Hydr. Eng.*, 112: 657-669.

- Blanckaert, K. and H.J. De-Vriend, 2003. Non-linear modeling of mean flow redistribution in curved open channels. *J. Water Resour. Res.*, 39: 1375-1375.
- Bodnar, T. and J. Prihoda, 2006. Numerical simulation of turbulent free-surface flow in curved channel. *J. Flow Turbulent Combust.*, 76: 429-442.
- De-Vriend, H.J., 1979. A mathematical model of steady flow in curve shallow channels. *J. Hydr. Res.*, 15: 37-54.
- De-Vriend, H.J. and H.J. Geoldof, 1983. Main flow velocity in Short River bends. *J. Hydr. Eng.*, 109: 991-1011.
- Engelund, F., 1974. Flow and bed topography in channel bends. *J. Hydraulics Division ASCE*, 100: 1631-1648.
- Henderson, F.M., 1966. *Open Channel Flow*. Macmillan Publishing Co. Inc., New York, ISBN-10: 0023535105, pp: 250-252.
- Hosseini, S.M. and J. Abrishami, 1999. *Open-Channel Hydraulics*. Emam Reza University, Mashhad, ISBN: 964-6882-19-21979.
- Leschziner, M.A. and W. Rodi, 1979. Calculation of strongly curved open channel flow. *J. Hydr. Division.*, 105: 1297-1314.
- Lien, H.C., T.Y. Hsieh, J.C. Yong and K.C. Yeh, 1999. Bend-flow simulation using 2D depth-averaged model. *J. Hydr. Eng.*, 125: 1097-1108.
- Mays, L.W., 1999. *Hydraulic Design Handbook*. McGraw-Hill Book Company, New York, ISBN: 0070411522.
- Molls, T. and H. Chaudhry, 1995. Depth-averaged open-channel flow model. *J. Hydr. Eng.*, 121: 453-465.
- Rozovskii, I.L., 1957. Flow of water in bends of open channels. Academy of Sciences of the Ukrainian SSR, Kiev, Israel Program for Scientific Translation, Jerusalem 1963.
- Shimuzu, Y., H. Yamaguchi and T. Itakura, 1990. Three-dimensional computation of flow and bed deformation. *J. Hydr. Eng.*, 116: 1090-1108.
- Steffler, P.M., N. Rajartnam and A.W. Peterson, 1985. Water surface change of channel curvature. *J. Hydr. Eng.*, 111: 866-870.
- Subramanya, K., 1982. *Flow in Open Channel*. McGraw-Hill Book Co., New Delhi, ISBN-10: 0074624466.
- USBR., 1985. *Design of Small Dams*. US Department of Interior Bureau of Reclamation, USA., ISBN-13: 978-0160033735.
- Ye, J. and J.A. McCorquadale, 1998. Simulation of curved open channel flow by 3D hydrodynamic model. *J. Hydr. Eng.*, 124: 687-698.